Radiation Physics and Chemistry 84 (2013) 105–110

Contents lists available at SciVerse ScienceDirect

Radiation Physics and Chemistry

journal homepage: www.elsevier.com/locate/radphyschem

Study of an alternative process for oxidizing Vapor Grown Carbon Nanofibers using electron beam accelerators

M.C. Evora [a,b,*], D. Klosterman [b,c], K. Lafdi [b,c], L. Li [c], L.G.A. Silva [d]

[a] Instituto de Estudos Avançados, São Jose dos Campos—SP, Brazil
[b] Chemical & Materials Engineering, University of Dayton, Dayton, OH 45469-0246, United States
[c] University of Dayton Research Institute (UDRI), Dayton, OH 45469-0160, United States
[d] Instituto de Pesquisas Energéticas e Nucleares (IPEN/CNEN-SP)Av. Prof. Lineu Prestes, 2242, Cidade Universitária, 05508000 São Paulo—SP, Brazil

ARTICLE INFO

Article history:
Received 1 January 2011
Accepted 1 January 2012
Available online 4 July 2012

Keywords:
Electron beam
Carbon nanofiber and oxidation

ABSTRACT

The use of a high-energy electron beam was explored in this study as an alternative technique for oxidizing vapor grown carbon nanofiber surfaces. The radiation exposures were carried out at three different electron beam facilities with beam energies of 1.5, 3.0 and 4.5 MeV and radiation doses ranging from 1000 to 3500 kGy. XPS analysis showed that oxygen was readily incorporated on the surface: the ratio O1s/C1s increased approximately by a factor of 4 when the carbon nanofibers were irradiated at 3500 kGy. The oxidized nanofibers exhibited better dispersion in a water/methanol solution (50% v/v) than as-received nanofibers. Raman spectroscopy revealed that the ID/IG ratios for most of the samples were statistically unchanged because the damage on the nanofiber surface was highly localized and did not lead to modifications on the bulk carbon nanofiber structure. The samples irradiated at higher dose rate exhibited significantly higher ID/IG ratios. The radiation process introduced defects on the graphene layers leading to a decrease of the decomposition onset temperatures up to 56 °C lower than the non-irradiated samples. Overall the results were repeatable across all facilities, illustrating the robustness of the process.

1. Introduction

The effects of ionizing radiation on carbon materials have been thoroughly investigated because of its importance in the fields of nuclear, medical, and materials science. Basically, the effect of ionizing radiation on carbon materials takes place as a displacement of carbon atoms from their amorphous or graphitic structures. For nanocarbon materials, only destructive effects were observed in early experiments involving bombardment of carbon nanotubes and fullerenes with ions. However, recent work reveals that radiation can exploit defect creation for novel materials development especially in electronic nanotechnology (Krasheninnikov and Banhat, 2007).

It is known that electron beam can be used to mechanically manipulate the interconnection of carbon nanostructures at high temperatures using TEM. For example, two crossing pristine tubes would not normally join, even at high temperatures, while e-beam irradiation has been observed to lead to cutting and welding of tubes and transformation of single wall nanotubes (SWNTs) to multiwall tubes (MWNTs) (Li and Banhart, 2004). The stability of nanotubes under electron irradiation is governed by generation and annealing of vacancies–interstitials pair. The interstitial defects have higher mobility and will determine the annealing process. Agglomeration of vacancies will lead to radiation cutting (Banhart et al., 2005). Also, radiation induces vacancies and the energy gained by dangling bond saturation can both weld tubes as well as allow for reaction with oxygen. This can contribute favorably to the nano-electronic structure because it may improve the electric conductivity for example. Previous studies have shown that making an electrically conductive connection between nanotubes is not straightforward. Instead of the desirable ohmic contacts, tunnel junctions are often generated with high resistance (Gupta et al., 2005; Krasheninnikov and Banhat, 2007; Zou et al., 2002; Banhart, 2001). For example, at high temperature a focused electron beam in a field emission transmission electron microscope (TEM) was able to transform local arrangements of SWNTs to MWNTs (Li and Banhart, 2004). Pregler and Sinnott, (2006) used computational molecular dynamic simulation to study electron beam modification of MWNTs. They concluded that electron beam is not surface limited and may lead to cross-links between inner layers.

Carbon nanofibers are being thoroughly investigated for application in structural composites in the aerospace industry.

* Corresponding author at: Instituto de Estudos Avançados, Km 5.5, São Jose dos Campos—SP, 12228001 Putim, Brazil. Fax: +55 1239441177.
E-mail address: cecilia@ieav.cta.br (M.C. Evora).

0969-806X/$ - see front matter © 2012 Elsevier Ltd. All rights reserved.
http://dx.doi.org/10.1016/j.radphyschem.2012.06.036

This will require careful control of the surface to promote properties required for end use because CNFs are not highly compatible with most polymers. Therefore, it is necessary to modify their surfaces through chemical or physical techniques to produce optimized polymer nanocomposites. Oxidizing the nanocarbon surface creates active sites, changing non-polar sites to polar compounds that are available for further chemical reaction or "grafting" (chemical reaction) with additional organic groups. Graphitic nanostructures show a variety of structural transformations under electron irradiation. For example, at ambient temperature, it may allow accumulation of defects and the structure may collapse. However, if the radiation is carried out above 300–400 °C, the mobility of atoms can be high enough to avoid this accumulation, and the structure can rearrange to new morphologies with desirable properties. The goal of the present study is to explore the potential of using e-beam radiation to oxidize CNF surfaces. To this end, CNF samples were exposed to different electron beam facilities at high levels of e-beam radiation doses in an atmosphere of air. The irradiated samples were analyzed by X-Ray Photoelectron Spectroscopy (XPS), Raman spectroscopy and Thermogravimetric Analysis (TGA) to assess the change to the surface and bulk mechanical properties.

2. Experimental

2.1. Raw materials

Pyrograf III™ Vapor Grown Carbon Nanofibers (VGCF) was purchased from Applied Science Inc. (Cedarville, Ohio). Many grades of VGCF are available, which differ in bulk density, wall architecture, overall diameter, and prior heat treatment. We selected the PR-25-PS-XT grade, which has an average diameter of 80 nm and has been heat treated in inert atmosphere up to 1100 °C to remove polyaromatic hydrocarbon and metal catalyst impurities from the surface. This grade has a good balance of mechanical and electrical properties. Compared to other grades of Pyrograf III, such as PR-24 and PR-19, the PR-25 grade has lower iron content, a smaller diameter, and a larger number of graphitic edge sites available along the length. A prior investigation was made with the VGCF PR-24-LHT-XT grade to verify the possibility of grafting oxygen functional groups onto it (Evora and Klosterman, 2007a, 2007b). The results showed little or no change in oxygen content. PR-24-LHT-XT has an average diameter of 100 nm, and it has been heat treated in inert atmosphere up to 1500 °C to increase the degree of graphitization compared to lower or non-heat treated versions such as PR-25-PS. In addition, the manufacturing process leads to formation of a CVD layer along the PR-24-LHT-XT external wall which can hinder the functionalization process by covering up graphitic end planes.

2.2. E-beam irradiation apparatus

2.2.1. University of Dayton Research Institute electron beam facility

Materials were irradiated with a pulsed linear accelerator operated by the University of Dayton Research Institute (Dayton, Ohio). Samples were placed on a steel platform below a linear scan horn as shown in Fig. 1. This equipment was operated with the following parameters: beam energy 3 MeV, pulse rate 150 pulses/s, pulse width 5 μs, pulse current 120 mA/pulse (equates to 0.09 mA time-averaged beam current), and air gap of 35 cm, resulting in a dose rate of approximately 16.7 kGy/min. The beam was spread over an area that was approximately constant in the *X* and *Y* directions for the irradiated samples. The details of the electron beam accelerator system are described in detail by Klosterman, (2003).

Fig. 1. Photograph of sample platform located inside shielded vault of e-beam facility.

As-received CNFs (PR-25-PS-XT) was irradiated in the form of a loose powder with bulk density of approximately 0.032 g/cm^3. PR-25-PS-XT loose powder was irradiated in air up to 3500 kGy. The samples were placed in an aluminum pan (21.5 cm × 11.5 cm × 6 cm) to a depth of 4 cm and heated on a hot plate up to 350 °C. The hot plate was then turned off and the radiation process was carried out.

Heating the samples was intended to provide higher mobility between atoms in the graphitic nanofiber walls. The goal was to increase the likelihood of displacing carbon atoms to enable the surface oxidation process. At ambient temperature, nanofibers can collapse easily due to high accumulation of defects. Increasing the temperature (via electron beam heating or external heating) increases the mobility of atoms and avoids this accumulation. The structure can rearrange itself to new morphologies with desirable properties (Banhart, 2006; Ritter et al., 2006).

2.2.2. Instituto de Pesquisas Energeticas e Nucleares (IPEN) electron beam facility

As-received PR-25-PS-XT was irradiated with a direct accelerator operated by the Instituto de Pesquisas Energetica e Nucleares (IPEN—Sao Paulo/Brazil). Samples in the form of a loose powder were placed on a steel platform below a linear scan horn. The samples were irradiated with an industrial electron accelerator Dynamitron, from radiation Dynamics Inc., model DC 1500/25-JOB 188 that was operated with the following parameters: beam energy 1.5 MeV, pulse current 3.36 mA, 7 kGy/pass with dose rate of 15.7 kGy/s.

The samples were placed in a sample holder of wood, and the PR-25-PS-XT powder was placed in small containers with 112 mm diameter to a depth of 4 mm. The samples were irradiated with 200, 1000, 2000 and 3500 kGy s. An external heat source was not used during this process because the high dose rate elevated the sample temperature around 200 °C due to the high dose rate. Carrying out the radiation process in a number of passes allowed the samples to cool between e-beam exposures and limit the upper temperature.

2.2.3. E-BEAM Services Inc. electron beam facility

As-received PR-25-PS-XT was irradiated with a direct accelerator operated by the E-BEAM Services Inc. (Lebanon,–Ohio, USA). Samples, as a loose powder, were placed on a steel platform below a linear scan horn. The samples were irradiated with a

150 kW Dynamitron manufactured by RDI (Radiation Dynamics Inc.) This equipment is a DC potential drop accelerator that was operated with the following parameters: beam energy 4.5 MeV, dose rate 15.7 kGy/s, dose history: 25 kGy/pass for 10 passes, 20 kGy/pass for 37 passes and 10 kGy/pass for 1 pass for a total dose of 1000 kGy. Samples were irradiated in air by placing loose powder in an aluminum pan (21.5 cm × 11.5 cm × 6 cm) to a depth of 4 cm. Another sample was irradiated in vacuum using a Mylar vacuum bag evacuated to about 25–25.5 in Hg of vacuum. The vacuum and open-air sample was irradiated at the same time one next to another.

2.3. Material analysis

The surface oxygen content of the nanofibers was characterized with X-ray Photoelectron Spectroscopy (XPS) analysis. A Surface Science Labs SSX-100 XPS spectrometer was used with a base pressure of 6×10^{-10} Torr in the analysis chamber, and an X-ray source with a 600 μm spot size. Samples were prepared by first drying the nanofibers in a vacuum oven overnight at 100 °C or higher, and then distributing a small amount of material on copper adhesive tape. Two areas were analyzed on each sample. Results are reported in terms of atom% oxygen in the form of single bonded oxygen (O–C), double bonded oxygen (O═C), single bonded nitrogen (N), and water (H_2O). The signals for single and double bonded oxygen are caused by groups that are covalently bonded to the nanofiber/tube wall, for example in the form or phenolic groups (–OH), aldehyde (–CHO), or carboxylic acid (–COOH). Water molecules would be attached by secondary bonding; especially hydrogen bonding in highly oxidized samples. The technique is sensitive only to surface atoms.

To verify modification in their graphitic structure, the samples were analyzed by Raman spectroscopy. Raman is a powerful physical technique that is commonly used to characterize carbon materials. It is a nondestructive technique and is sensitive to the surface modifications occurring in graphitized carbon structures. A Renishaw 1000 micro-Raman Spectrometer with an Ar+ ion laser at 514 nm (2.14 eV) was used. Incident and scattered beams were focused with a 50× objective lens and laser spots with resolutions as low as 2 μm and a spectrum range between 100 and 5000 cm^{-1}. The samples were analyzed in form of a thin paper (around 20 μm) to reach more accurate results. The papers were prepared the same way as described above. Twelve measurements were made on different areas of each sample to provide statistically significant results.

The thermal and thermo-oxidative stability of the samples were characterized with Thermogravimetric Analysis (TGA) using a TA Instruments Q5000 unit. Both air and pure nitrogen atmospheres were used, with a heating rate of 10 °C/min from 25 to 1000 °C; the sample weight was around 3.5 mg. Lower degradation temperature may indicate that some damage was introduced on the nanofiber surface, and it can be an indicative of cutting and oxidation caused by the radiation process.

3. Results and discussion

3.1. XPS results

XPS results are presented in Table 1.

The results given by XPS analysis showed that the ratio O1s/C1s increased approximately by a factor of 3 when the PR-25-PS was irradiated at 3500 kGy in the UDRI facility and a factor of 4.3 for the sample irradiated in the IPEN facility. The relative amount of carbon bonded to oxygen-containing groups increased, indicating that oxygen reacted with the carbon nanofiber surface and modified the carbon nanofiber structure. The only further detail from XPS results was that both carbon oxygen bonds (C–O) and carbonyl (C═O) increased, which may be related to carboxylic acid. Further investigation would be necessary to verify specifically which oxygen functional groups were predominant and is beyond the scope of this work. Generally, the types of oxygen functional groups introduced to the surface are a strong function of the oxidation process used. For example, Zhou et al. (2007) showed that the amount and distribution of surface oxygen complexes on carbon nanofibers varied with different chemical and thermal treatments. The current research will focus on using radiation process to oxidize carbon nanofibers surface.

Table 1
XPS results of non-irradiated and irradiated samples showing the oxygen/carbon ratio.

Dose	XPS—O1s/C1s		
	UDRI[a]	IPEN	E-BEAM Services
Non-irradiated (non-heated)	0.03	0.03	0.03
200 kGy in air	–	0.04	–
1000 kGy in air	0.08	0.08	0.07
2000 kGy in air	–	0.10	–
3500 kGy in air	0.09	0.13	–
1000 kGy in vacuum	–	–	0.02

[a] Evora et al. (2010).

3.2. Raman results

Raman spectroscopy is very sensitive to the breakdown in translational symmetry of carbon materials and can supply some detailed quantitative information about the microstructure. Generally the Raman spectra of carbon materials are simple, with the two most intense bands between 1000 and 2000 cm^{-1}. The dispersion of π electrons in graphene is why Raman spectroscopy is always resonant for carbon. However, Raman has some drawbacks that may lead to misinterpretation of the spectra. Ferrari investigated the impact of multiple layers of graphene on the D band of Raman spectrum (Yang et al., 2009; Ferrari, 2007). For more than 5 layers, the D band of Raman spectrum becomes hardly distinguishable from the bulk graphite. Thus Raman spectroscopy can clearly identify less than 5 graphene layers. Ferrari also pointed out that the same sample can have a G peak with different positions and different values for full-width at half-mean (FWHM).

The Raman spectra results are summarized in Table 2 and presented in Figs. 3 and 4. In general, the Raman results showed that there were no statistically significant change of ID/IG ratios, and the shapes and intensities of D and G bands in the spectrum of non-irradiated nanofibers were not much different from those of irradiated ones. Thus, there was no indication of damage to the microstructure. Some change was noticed in the sample irradiated at IPEN facilities. The IPEN electron beam facility carried out process with very high radiation dose rate (15.7 kGy/s) leading to higher beam heating due to less time for heat transfer away from the sample. Higher mobility of the atoms in the graphene layers and an immediate recombination process may have allowed for more diffusion of oxygen into the carbon nanofiber structure, but this process was not able to damage the bulk PR-25-PS structure.

The radiation damage was localized to the surface and did not compromise the core of the carbon nanofiber. Thus, the advantage of this process is that the overall graphitic structure has not been damaged. The electron beam interacts with the external layer, which is less organized than the bulk of the wall. Raman spectroscopy is a bulk characterization technique in which the laser

Table 2
Raman results of PR-25-PS irradiated at various facilities showed the D and G peak frequency and their ratio.

	Non-irradiated	1000 kGy in air	2000 kGy in air	3500 kGy in air	1000 kGy in vacuum
UDRI[a]					
ID/IG	3.67 ± 0.07	3.70 ± 0.10	–	3.72 ± 0.09	–
D frequency (cm^{-1}	1350.72 ± 1.06	1352.41 ± 0.94	–	1351.83 ± 0.9	–
G frequency (cm^{-1})	1590.80 ± 1.5	1590.22 ± 1.09	–	1590.37 ± 1.03	–
IPEN					
ID/IG	3.63 ± 0.06	3.75 ± 0.1	3.88 ± 1.17	3.82 ± 0.08	–
D frequency (cm^{-1})	1351.3 ± 0.99	1352 ± 0.68	1352.40 ± 0.85	1354.10 ± 1.00	–
G frequency (cm^{-1})	1591.4 ± 1.2	1591.6 ± 0.78	1591.4 ± 0.84	1592.10 ± 0.48	–
E-BEAM service					
ID/IG	3.70 ± 0.08	3.73 ± 0.07	–	–	3.68 ± 0.06
D frequency (cm^{-1})	1350.9 ± 0.67	1351.35 ± 0.89	–	–	1351.50 ± 1.12
G frequency (cm^{-1})	1590.18 ± 1.36	1590.11 ± 1.37	–	–	1591.46 ± 1.47

[a] Evora et al. (2010).

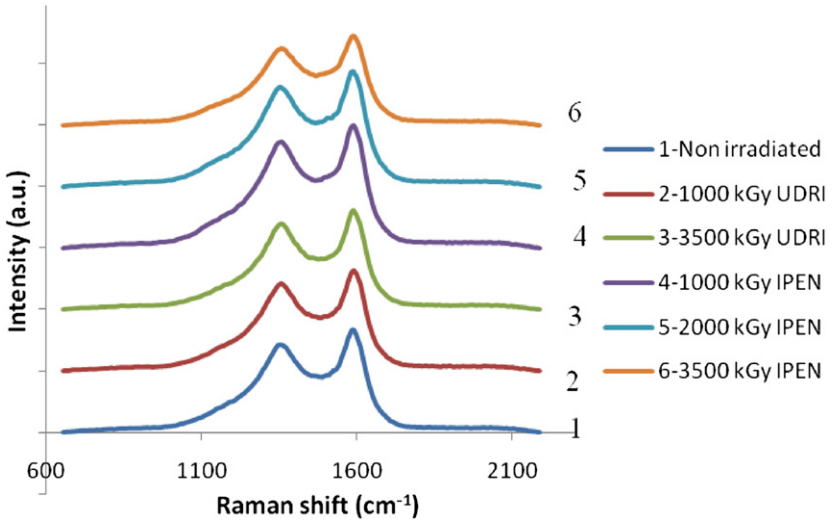

Fig. 2. Raman spectroscopy results for PR-25-PS powder irradiated in UDRI Evora et al. (2010) and IPEN facilities.

penetration (~1 μm) (Darmstadt et al., 1997) exceeds the thickness of the turbostratic carbon layer deposited on the nanofiber surface where the oxidation takes place. In general, the graphite structure of the nanofiber core did not show any damage.

In Fig. 2 the Raman curves of samples irradiated in two different electron beam facilities are presented. The samples irradiated at 1000 and 2000 kGy in IPEN exhibit a slightly higher intensity D and G band than for UDRI. The E-BEAM Services Raman curves for sample irradiated in air at 1000 kGy s presented in Fig. 3 also had slight higher intensity compared to the ones irradiated at 1000 kGy s in vacuum and non-irradiated samples. The small increasing of the D and G band indicates that the e-beam process carried out in air not only induces some defects on carbon nanofiber walls related to oxygen attachment and a possible change in graphitic order, but also further removes some amorphous carbon.

3.3. TGA results

The onset degradation temperature results for the electron beam irradiated samples are presented in Table 3. It shows that the irradiated samples degraded at lower temperature. For instance, the decomposition onset temperatures for the samples irradiated at 3500 kGy at UDRI and IPEN facilities were 13 °C (Evora et al., 2010) and 56 °C lower than the non-irradiated samples respectively. The reason for the decrease of onset degradation temperature is that the radiation process introduced

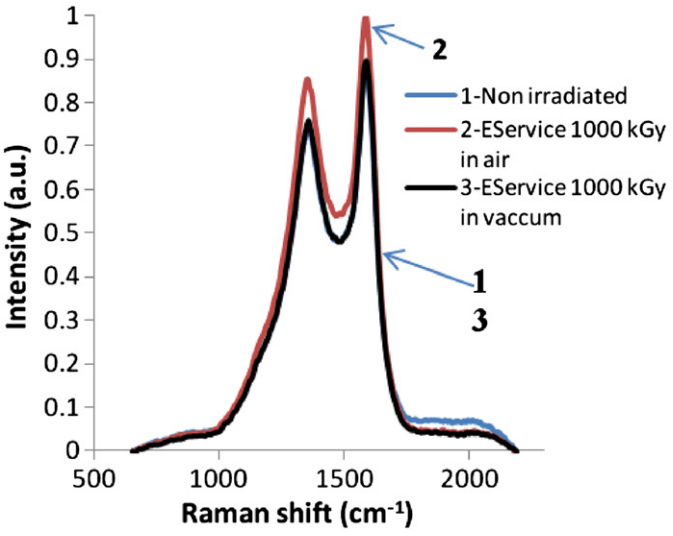

Fig. 3. Raman spectroscopy results for PR-25-PS powder irradiated in air and in vacuum at E-BEAM Services facility.

defects on the graphene layers structure. The samples irradiated with higher dose rate (IPEN) at 1000 kGy showed higher decrease of onset degradation temperature.

Table 3
Onset degradation temperature for sample irradiated in UDRI and IPEN facilities at different doses.

Dose	TGA—onset degradation temperature (°C) (10 °C/min in air)	
	UDRI[a]	IPEN
Non-irradiated (non-heated)	572	556
200 kGy in air	–	556
1000 kGy in air	558	517
2000 kGy in air	–	506
3500 kGy in air	559	500

[a] Evora et al. (2010).

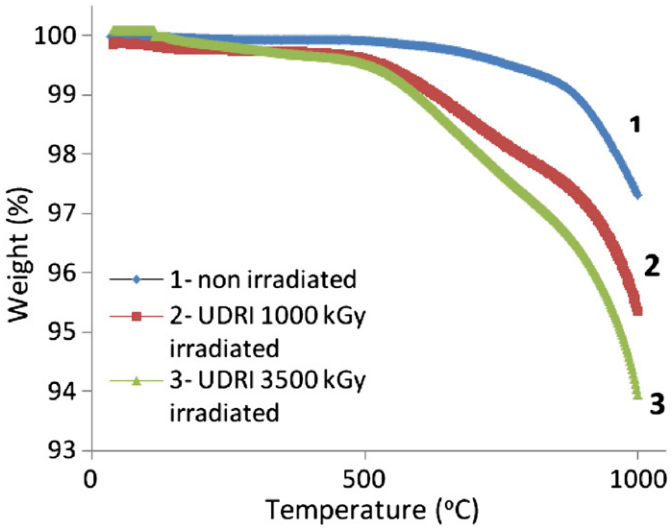

Fig. 4. TGA results of UDRI irradiated PR-25-PS (10° C/min in nitrogen).

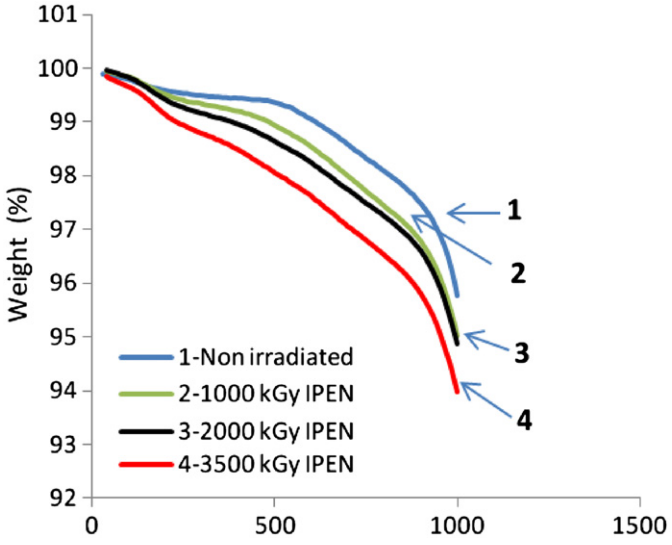

Fig. 5. TGA results of IPEN irradiated PR-25-PS (10 °C/min in nitrogen).

The TGA results for electron beam irradiated samples heated under nitrogen atmosphere are given in Figs 4 and 5 (Evora et al., 2010) indicating that the thermal stability of non-irradiated PR-25-PS was higher than the irradiated ones. This stability can be attributed to a variety of factors, including length/diameter and the size distribution, degree of defects and damages. The non-irradiated sample (0 kGy) began to lose mass around 600 °C, which was attributed to impurities or imperfections in the nanofiber. A distinct weight loss occurred around 200–500 °C for the irradiated samples. In addition, the irradiated samples exhibited a more pronounced weight loss from 500 to 1000 °C than non-irradiated nanofibers, although the final weight loss was still fairly low. This was not surprising given that the total amount of surface oxidation (~2.4 atom%) comprises a very small fraction of the total mass of the nanofiber. Overall, the samples irradiated to 1000 kGy and 3500 kGy showed a higher total mass loss by a factor of 1.7 and 2.2, respectively compared to non-irradiated.

The extra weight loss and lower onset degradation temperature were attributed to the higher amount of non-graphitic carbon in the irradiated samples due to the oxidation process. Non-graphitic carbon is inherently less thermally stable than graphitic carbon. The radiation has generated more defects and higher surface area that increase carbon oxidation reaction.

4. Conclusions

The results presented in this study represent an alternative way to modify the surface of nanofibers via electron beam. The reproducibility of the oxidation process using different types of electron beam facilities was verified by XPS, Raman and TGA. The carbon nanofibers irradiated in air experienced the creation of free radicals on the nanofiber surface by e-beam knock-on damage which lead to vacancies and other point defects. These produced a very energetic surface that enhanced bonding with polar media. When the e-beam interacted with the carbon structure in an oxidative environment (O2, H2O), the carbon surface oxidized to CO and CO2. Additional research is needed to investigate more closely the effects of key parameters such as power of exposure, temperature, time, and atmosphere.

Acknowledgments

The authors wish to thank CAPES/Fulbright for Ms. Evora's fellowship and FAPESP for financial support. Also we would like to thank Mr. Tom Wittberg from UDRI for performing XPS testing and analysis, Mr. Dave Keenan from E-BEAM Services and Mrs. Somessari and Carlos Gaia from IPEN for irradiating the samples.

References

Banhart, F., 2001. The formation of connection between carbon nanotubes in an electron beam. Nano Lett. 1 (6), 329–332.
Banhart, F., 2006. Irradiation of carbon nanotubes with a focused electron beam in the electron microscope. J. Mater. Sci. 41, 4505–4511.
Banhart, F., Jixue, L., Terrones, M., 2005. Cutting single-walled carbon nanotubes with an electron beam: evidence for atom migration inside nanotubes. Small J. 1 (10), 953–956.
Darmstadt, H., Summchem, L., Ting, J.M., Roland, U., 1997. Effect of surface treatment on the bulk chemistry and structure of vapor grown carbon fibers. Carbon 35, 1581–1585.
Evora, M.C., Klosterman, D., Lafdi, K., Li, L., Abot, J.L., 2010. Functionalization of carbon nanofibers through electron beam irradiation. Carbon 48, 2037–2046.
Evora, M.C., Klosterman, D., 2007a. Use of electron beam irradiation for surface functionalization of carbon nanofiber. In: SAMPE Proceedings. Cincinnati, Ohio.
Evora, M.C., Klosterman, D., 2007b. Use of electron beam irradiation for surface functionalization of carbon nanofiber. In: SAMPE Proceedings. Baltimore, Maryland.
Ferrari, A., 2007. Raman spectroscopy of graphene and graphite: disorder, electron–phonon coupling, doping and nanodiabatic effect. Solid State Commun. 143, 47–57.
Gupta, S., Patel, R.J., Smith, N.D., 2005. Advanced carbon-based materials as space radiaton shield. Mater. Res. Soc. Symp. Proc. 851, 1–7.
Klosterman, D., 2003. Characteristics of an electron beam used for basic research studies on composite curing, In: SAMPE Proceedings. Long Beach, CA.

Krasheninnikov, A.V., Banhat, F., 2007. Engineering of nanostructured carbon materials with electron or ion beams. Nat. Mater. 6, 723–733.
Li, J., Banhart, F., 2004. The engineering of hot carbon nanotubes with a focused electron beam. Nano Lett. 4 (6), 1143–1146.
Pregler, S.K., Sinnott, S.B., 2006. Molecular dynamics simulations of electron and ion beam irradiation of multiwalled carbon nanotubes: the effect on failure by inner tube sliding. Phys. Rev. B 73, 224106.
Ritter, U., Scharff, P., Siegmund, C., 2006. Radiation damage to multi-walled carbon nanotubes and their Raman vibrational modes. Carbon 44, 2694–2700.
Yang, K., Gu, M., Guo, Y., Pan, X., Mu, G., 2009. Effect of carbon nanotube functionalization on mechanical and thermal properties of epoxy composites. Carbon 47, 1723–1737.
Zhou, J., Sui, Z., Zhu, J., Cen, D., Dai, Y., Yuan, W., 2007. Characterization of surface oxygen complexes on carbon nanofibers by TDP, XPS and FT-IR. Carbon 45, 785–796.
Zou, H., Yang, Y., Li, Q., Zhang, J., Liu, Z., 2002. Electron beam- induced structure transformation of single-walled carbon nanotubes. Carbon 40, 2263–2284.